

Supporting Information

Isomer engineering of the dipyrido[3,2-*a*:3',4'-*c*]phenazine acceptor based red thermally activated delayed fluorescent emitters

*Shantaram Kothavale, Won Jae Chung, Jun Yeob Lee**

*School of Chemical Engineering, Sungkyunkwan University
2066, Seobu-ro, Jangan-gu, Suwon, Gyeonggi, 440-746, Korea*

E-mail: leej17@skku.edu

Table of contents

Figure. S1. DFT optimized structures of *o*DMAC-DPPZ and *p*DMAC-DPPZ with their dihedral angles between DMAC donor and DPPZ acceptor unit.

Figure. S2. Fluorescence and phosphorescence spectra of *o*DMAC-DPPZ and *p*DMAC-DPPZ at 77 K in toluene solvent.

Figure S3. Thermogravimetric analysis (TGA) curves of *o*DMAC-DPPZ and *p*DMAC-DPPZ TADF emitters.

Figure S4. Cyclic voltammogram (CV) curves of *o*DMAC-DPPZ and *p*DMAC-DPPZ TADF emitters.

Figure. S5. Current density–voltage–luminance (J–V–L) curves of *o*DMAC-DPPZ and *p*DMAC-DPPZ at 1 % doping concentration.

Figure. S6. EQE–luminance curves of *o*DMAC-DPPZ at 1, 3 and 5 % doping concentration.

Figure. S7. EQE–luminance curves of *p*DMAC-DPPZ at 1, 3 and 5 % doping concentration.

Figure. S8. EL spectra of *o*DMAC-DPPZ at 1, 3 and 5 % doping concentration.

Figure. S9. EL spectra of *p*DMAC-DPPZ at 1, 3 and 5 % doping concentration.

Figure. S10. Fluorescence (PL) and phosphorescence (LTPL) spectra of DPPZ acceptor unit in toluene solvent.

Figure S11. ^1H NMR spectrum of intermediate 1.

Figure S12. ^{13}C NMR spectrum of intermediate 1.

Figure S13. ^1H NMR spectrum of intermediate 3.

Figure S14. ^{13}C NMR spectrum of intermediate 3.

Figure S15. ^1H NMR spectrum of *o*DMAC-DPPZ.

Figure S16. ^{13}C NMR spectrum of *o*DMAC-DPPZ.

Figure S17. ^1H NMR spectrum of *p*DMAC-DPPZ.

Figure S18. ^{13}C NMR spectrum of *p*DMAC-DPPZ.

Experimental

General information

4,5-Difluorobenzene-1,2-diamine and 9,9-dimethyl-9,10-dihydroacridine were purchased from P&H tech. *p*-toluenesulphonic acid (PTSA), palladium acetate (Pd(OAc)₂) and sodium tert-butoxide (NaOt-Bu) were purchased from Alfa Aesar Co. Caesium carbonate (Cs₂CO₃), anhydrous ethanol, *N,N*-Dimethylformamide (DMF), anhydrous toluene, acetic acid and zinc metal were obtained from Duksan Sci. Co. All these chemicals were used without further purification. Column chromatography (Silica Gel 60, 230–400 mesh, Merck) purified both the TADF emitters were further purified by sublimation (10⁻³ Torr at 300 °C) before applying for OLED devices. The ultraviolet-visible (UV-vis) absorption spectra and photoluminescence (PL) spectra were recorded using UV-vis spectrophotometer (JASCO, V-730) and fluorescence spectrophotometer (PerkinElmer, LS-55) respectively. CV measurement was carried out using Ivium Tech., Iviumstat instrument in dichloromethane solution with scan rate at 100 mV/s. The glassy carbon, platinum wire and Ag/AgCl were used as working, counter and reference electrode respectively. Internal standard was ferrocenium/ferrocene couple and supporting electrolyte was 0.1 M tetrabutylammonium perchlorate (TBAClO₄). Absolute photoluminescence quantum yields (PLQYs) of 1 wt % doped polystyrene film were measured with a Hamamatsu Quantaaurus-QY C11347-11 spectrometer and the transient photoluminescence decay characteristics of solid film samples were recorded using a Quantaaurus-Tau fluorescence lifetime measurement system (C11367-31, Hamamatsu Photonics). The ¹H and ¹³C nuclear magnetic resonance (NMR) spectra were recorded on a Avance-500 (Bruker, 500 MHz) spectrometer using deuterated chloroform (CDCl₃) solvent. Chemical shifts of the ¹H and ¹³C NMR signals were quoted relative to tetramethylsilane (δ = 0.00). All coupling constants are reported in Hertz. The mass spectra were recorded using a Advion, Expression LCMS spectrometer in APCI mode. TD-DFT calculations was carried out using the Gaussian 09 package and Becke's three parameter exchange functional B3LYP with basis set of 6-31G (d).

Synthesis of 11,12-difluorodipyrido[3,2-a:2',3'-c]phenazine (1)

1,10-Phenanthroline-5,6-dione (2 g, 9.51 mmol) and 4,5-difluorobenzene-1,2-diamine (1.37 g, 9.51 mmol) were dissolved in acetic acid (50 mL) and the resulting mixture was stirred at 110 °C for 12 h. After cooling to room temperature, a yellow solid precipitated out was filtered, washed

with n-hexane and dried well as a pure product (2.6 g, 86 %). ¹H NMR (500 MHz, CDCl₃): δ 9.44-9.46 (dd, *J* = 8 and 1.5 Hz, 2H), 9.25-9.26 (d, *J* = 4.5 Hz, 2H), 7.97-8.01 (t, *J* = 9 Hz, 2H), 7.74-7.76 (q, 2H). ¹³C NMR (126 MHz, CDCl₃) δ 154.5, 154.4, 153.1, 152.5, 152.3, 148.5, 141.2, 140.1, 139.9, 139.9, 133.8, 127.1, 124.4, 114.9, 114.8, 114.7. MS (FAB) *m/z* 934 [(M + H)⁺].

Synthesis of 11,12-bis(9,9-dimethylacridin-10(9H)-yl)dipyrido[3,2-a:2',3'-c]phenazine (oDMAC-DPPZ)

Intermediate 1 (0.6 g, 1.88 mmol) and 9,9-Dimethyl-9,10-dihydroacridine (1.18 g, 5.65 mmol) were dissolved in DMF (20 mL); Cs₂CO₃ (2.45 g, 7.54 mmol) was added and the reaction mixture was heated in sealed tube at 180 °C for 24 hrs. After cooling to room temperature, water was added in the reaction mixture. The solid precipitated out was filtered and dried well. The crude product obtained was further purified by column chromatography (2 % MeOH in DCM) to afford desired product as red solid (0.24 g, 55.81 %). ¹H NMR (500 MHz, CDCl₃): δ 9.66-9.68 (d, *J* = 7.5 Hz, 2H), 9.32-9.33 (d, *J* = 3.5 Hz, 2H), 8.82 (s, 2H), 7.82-7.85 (m, 2H), 7.25-7.27 (m, 4H), 6.77-6.80 (t, *J* = 7.5 Hz, 4H), 6.70-6.73 (t, *J* = 7 Hz, 4H), 6.55-6.56 (d, *J* = 8 Hz, 4H), 1.25 (s, 12H). ¹³C NMR (126 MHz, CDCl₃) δ 153.3, 148.9, 143.4, 142.6, 142.4, 139.4, 136.6, 134.3, 130.5, 127.6, 126.0, 125.9, 124.7, 121.3, 114.7, 35.8, 29.9. MS (FAB) *m/z* 934 [(M + H)⁺].

Synthesis of 3,6-bis(9,9-dimethylacridin-10(9H)-yl)benzene-1,2-diamine(3)

Intermediate 2 (1.6 g, 2.90 mmol) was dissolved in acetic acid (30 mL), zinc (1.9 g, 29 mmol) was added slowly and the mixture was refluxed for 4-5 hrs. After cooling to room temperature unreacted zinc metal was removed by filtration. Water was added and the solid precipitated out was filtered and dried well to afford as pure product (1.1 g, 72.84 %). ¹H NMR (500 MHz, CDCl₃): δ 7.51-7.52 (d, *J* = 8 Hz, 4H), 7.10-7.13 (t, *J* = 8 Hz, 4H), 6.98-7.01 (t, *J* = 7.5 Hz, 4H), 6.89 (s, 2H), 6.51 (s, 2H), 6.52 (s, 2H), 1.76 (s, 6H), 1.71 (s, 6H). ¹³C NMR (126 MHz, CDCl₃) δ 139.2, 135.8, 130.5, 127.2, 127.1, 125.9, 122.9, 121.3, 113.8, 36.2, 32.59, 31.6. MS (FAB) *m/z* 934 [(M + H)⁺].

Synthesis of 10,13-bis(9,9-dimethylacridin-10(9H)-yl)dipyrido[3,2-a:2',3'-c]phenazine (pDMAC-DPPZ)

Intermediate 3 (0.5 g, 0.95 mmol) and 4,5-difluorobenzene-1,2-diamine (0.2 g, 0.95 mmol) were dissolved in acetic acid (20 mL) and the resulting mixture was stirred at 120 °C for 12 h. After cooling to room temperature, a dark red colored solid precipitated out was filtered, washed with n-hexane and dried well. The crude product obtained was further purified by column chromatography (3 % MeOH in DCM) to obtain dark red solid as pure product (0.41 g, 62.12 %). ¹H NMR (500 MHz, CDCl₃): δ 9.11-9.12 (d, *J* = 3.5 Hz, 2H), 8.90-9.01 (d, *J* = 8 Hz, 2H), 8.27 (s, 2H), 7.61-7.63 (d, *J* = 7.5 Hz, 4H), 7.50-7.52 (m, 2H), 6.93-7.00 (m, 8H), 6.32-6.34 (d, *J* = 8 Hz, 4H), 1.97 (s, 12H). ¹³C NMR (126 MHz, CDCl₃) δ 153.1, 148.8, 142.3, 142.1, 141.3, 139.7, 135.2, 134.4, 130.5, 126.7, 125.8, 124.4, 121.2, 114.3, 36.5, 32.1. MS (FAB) *m/z* 934 [(M + H)⁺].

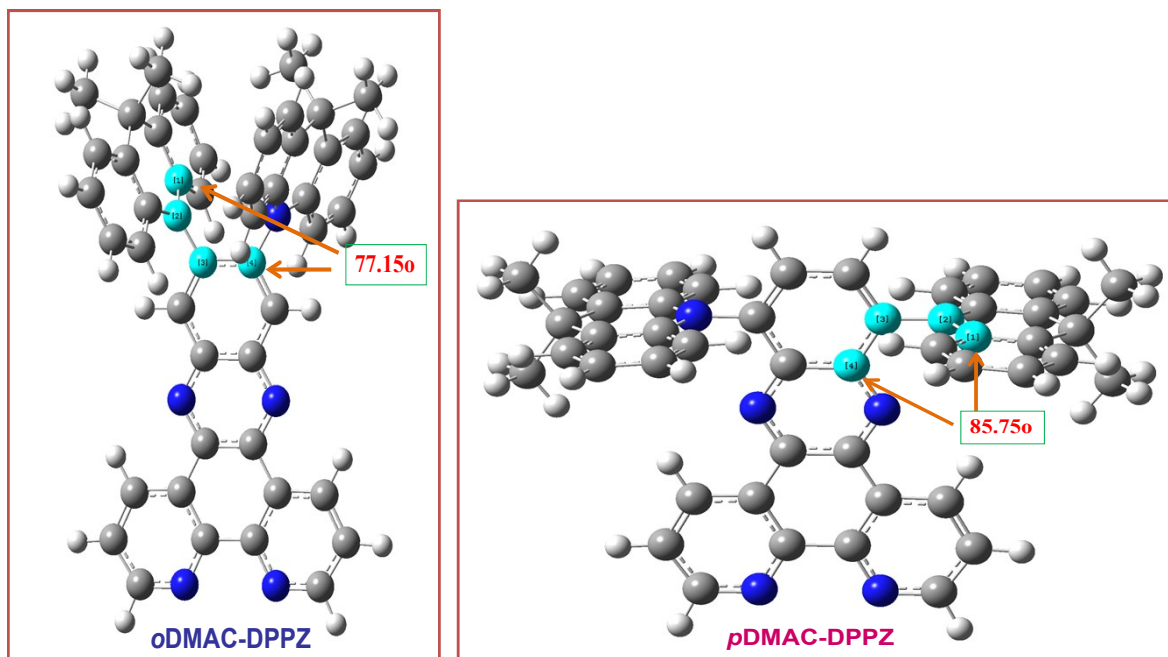


Figure. S1. DFT optimized structures of *o*DMAC-DPPZ and *p*DMAC-DPPZ with their dihedral angles between DMAC donor and DPPZ acceptor unit.

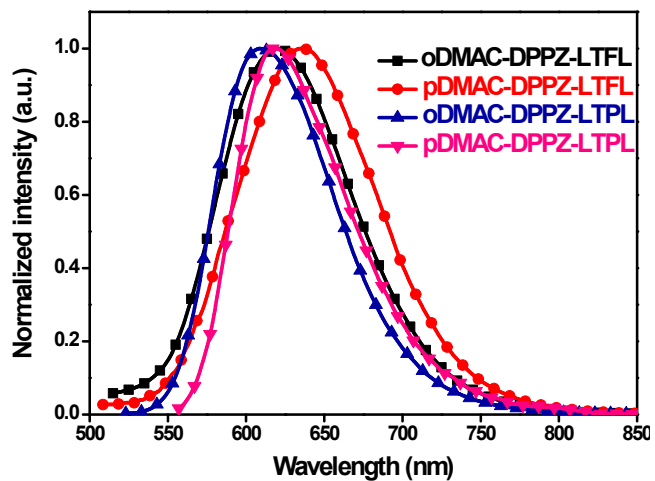


Figure. S2. Fluorescence and phosphorescence spectra of *o*DMAC-DPPZ and *p*DMAC-DPPZ at 77 K in toluene solvent.

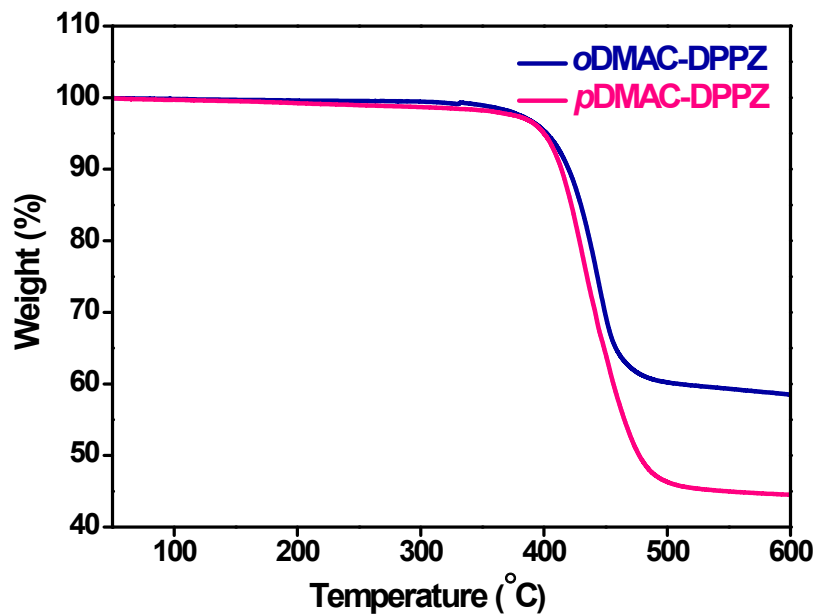


Figure S3. Thermogravimetric analysis (TGA) curves of *o*DMAC-DPPZ and *p*DMAC-DPPZ TADF emitters.

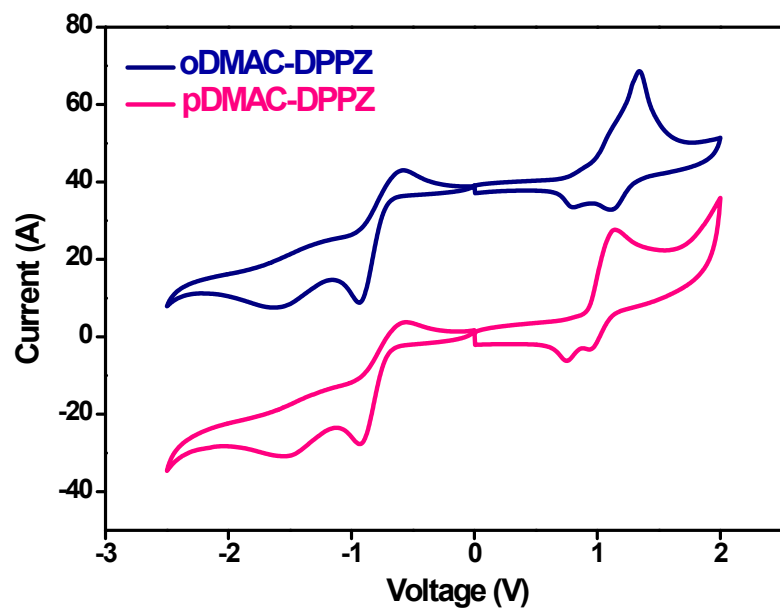


Figure S4. Cyclic voltammograms (CV) curves of *o*DMAC-DPPZ and *p*DMAC-DPPZ TADF emitters.

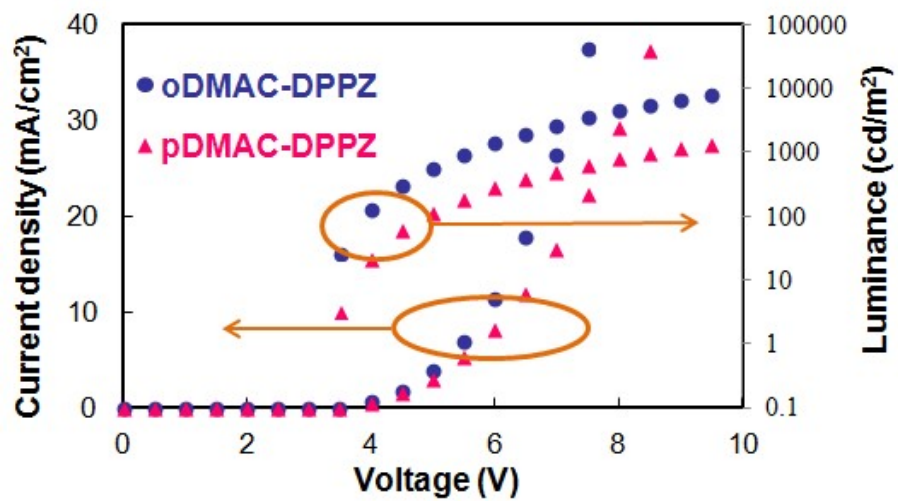


Figure. S5. Current density–voltage–luminance (J–V–L) curves of *o*DMAC-DPPZ and *p*DMAC-DPPZ at 1 % doping concentration.

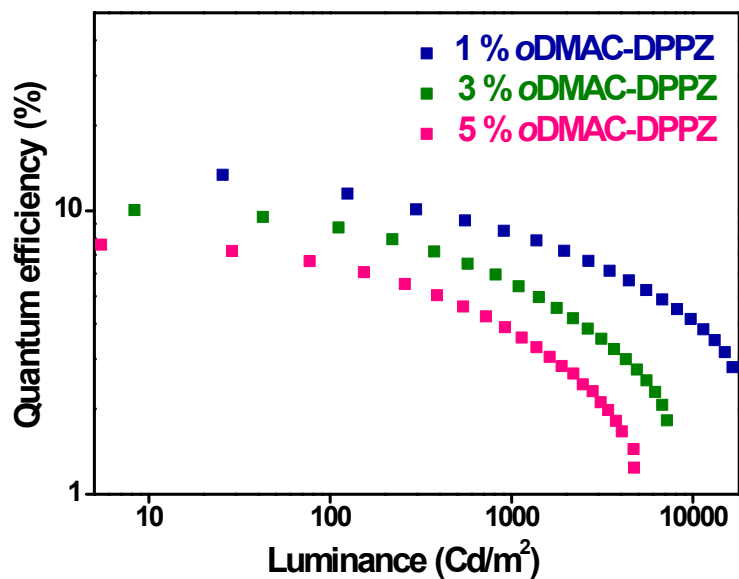


Figure. S6. EQE–luminance curves of *o*DMAC-DPPZ at 1, 3 and 5 % doping concentration.

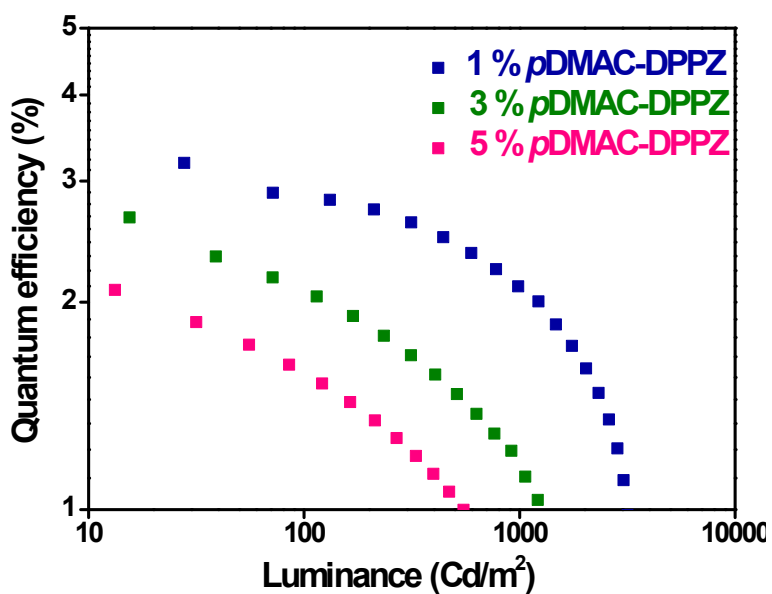


Figure. S7. EQE–luminance curves of *p*DMAC-DPPZ at 1, 3 and 5 % doping concentration.

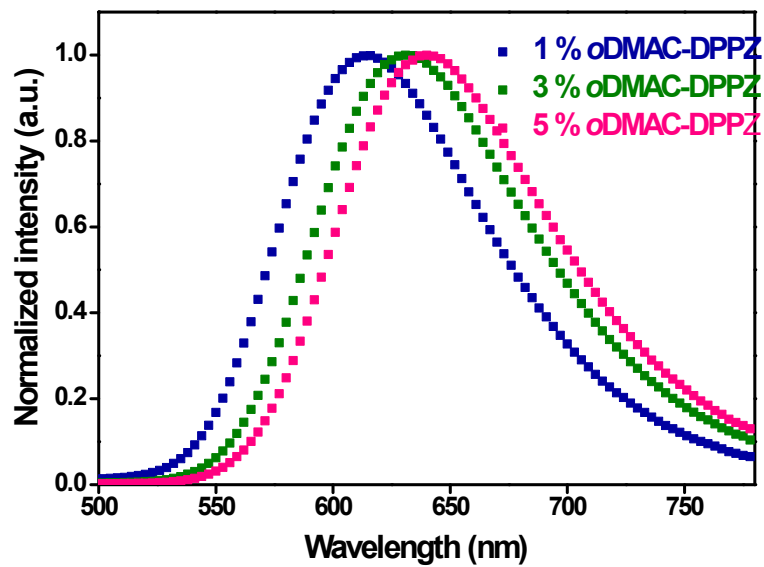


Figure. S8. EL spectra of *o*DMAC-DPPZ at 1, 3 and 5 % doping concentration.

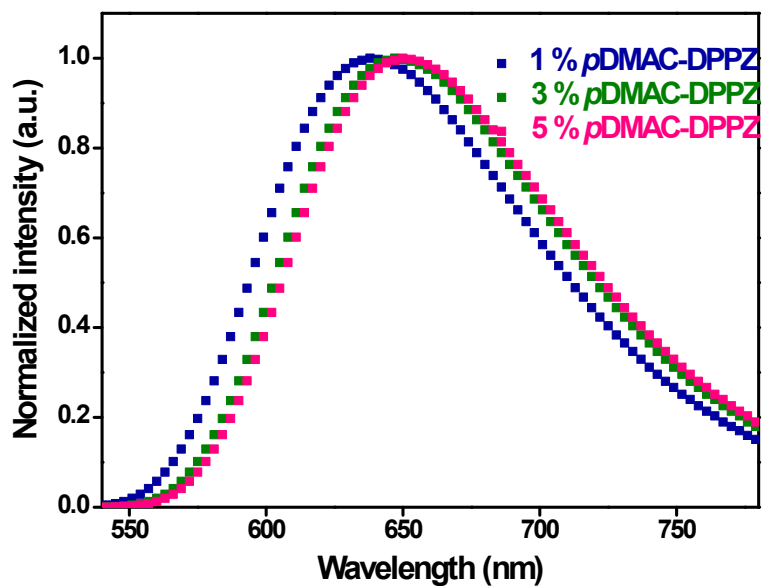


Figure. S9. EL spectra of *p*DMAC-DPPZ at 1, 3 and 5 % doping concentration.

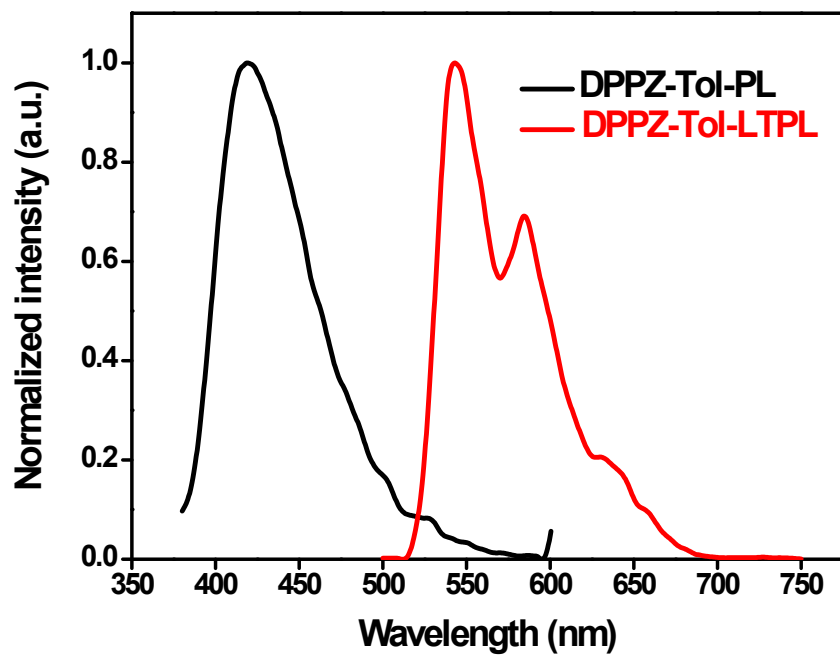


Figure. S10. Fluorescence (PL) and phosphorescence (LTPL) spectra of DPPZ acceptor unit in toluene solvent.

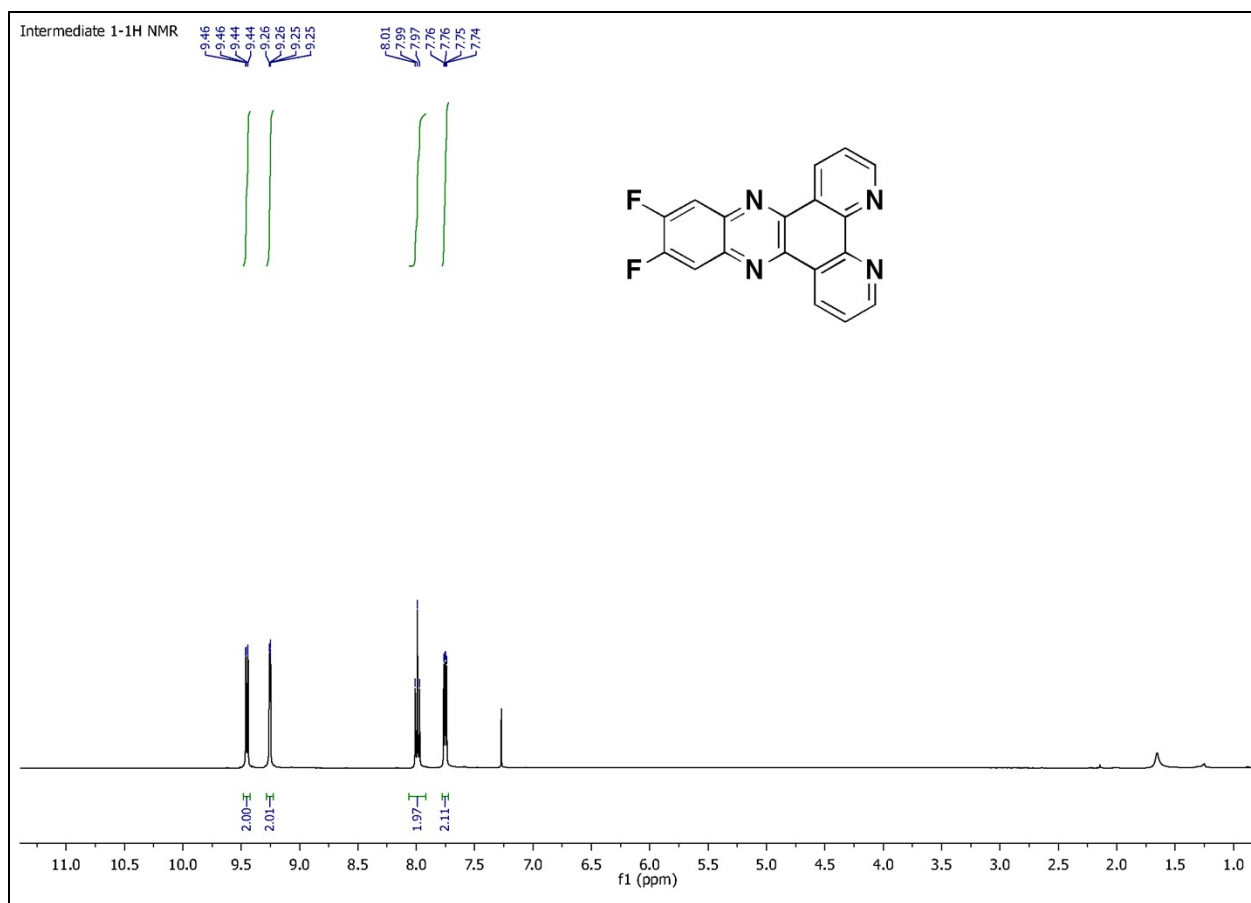


Figure S11. ¹H NMR spectrum of intermediate 1.

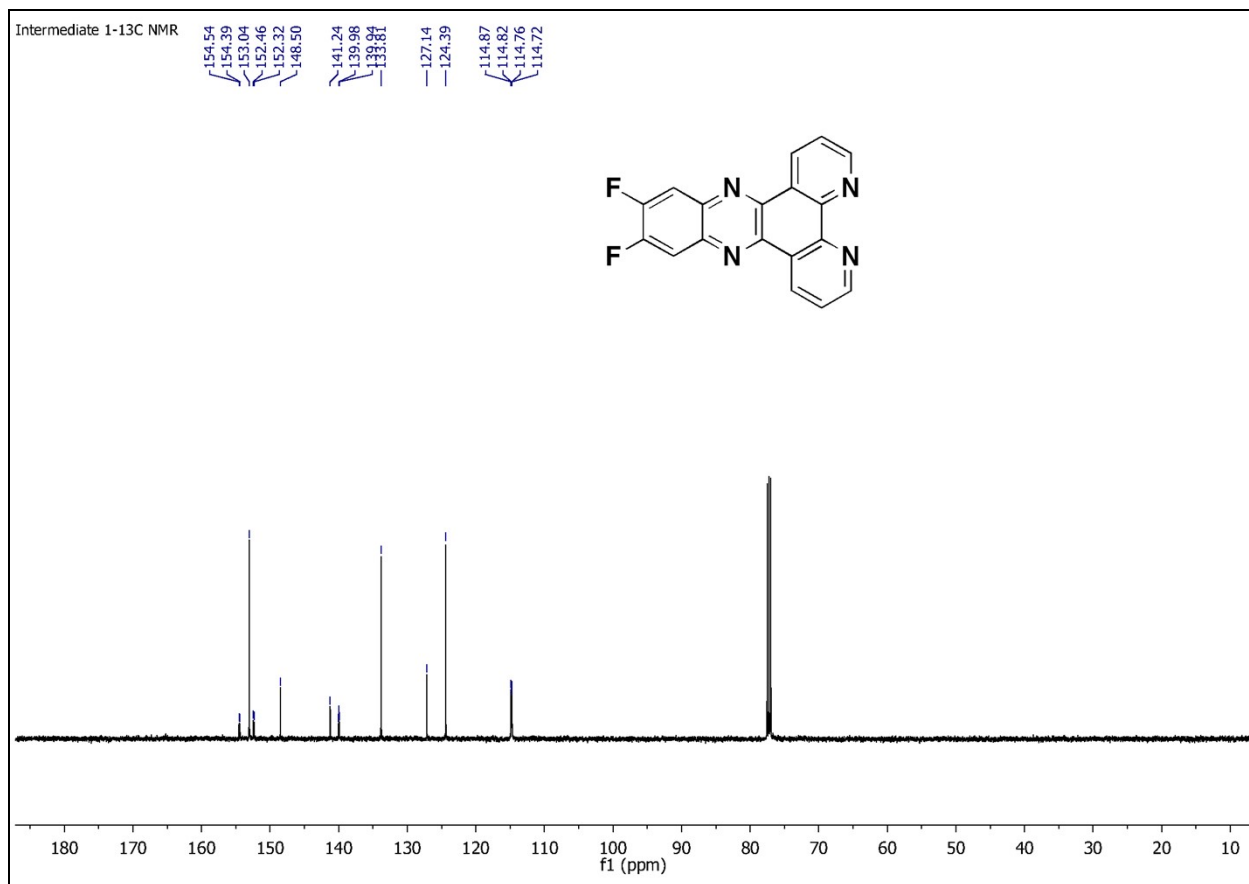


Figure S12. ¹³C NMR spectrum of intermediate 1.

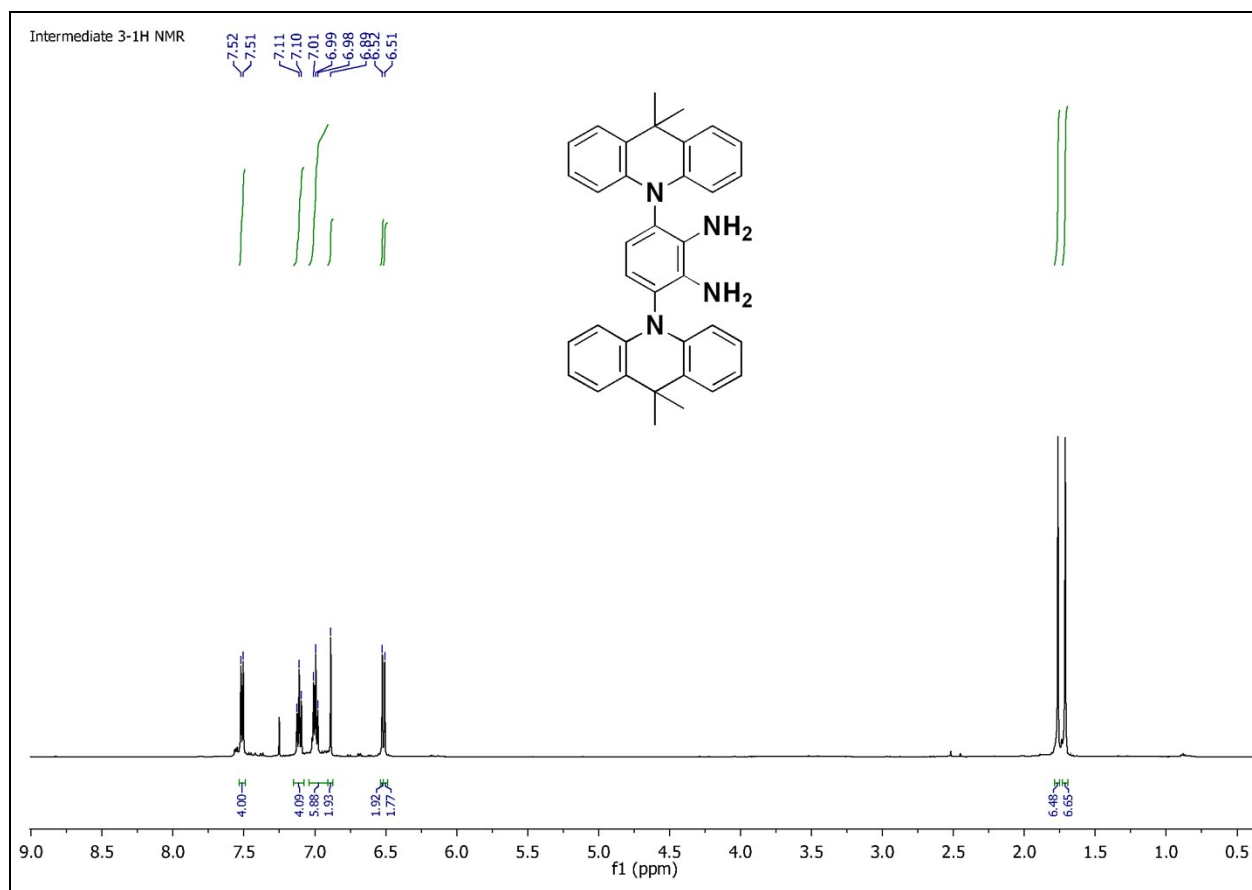


Figure S13. ^1H NMR spectrum of intermediate 3.

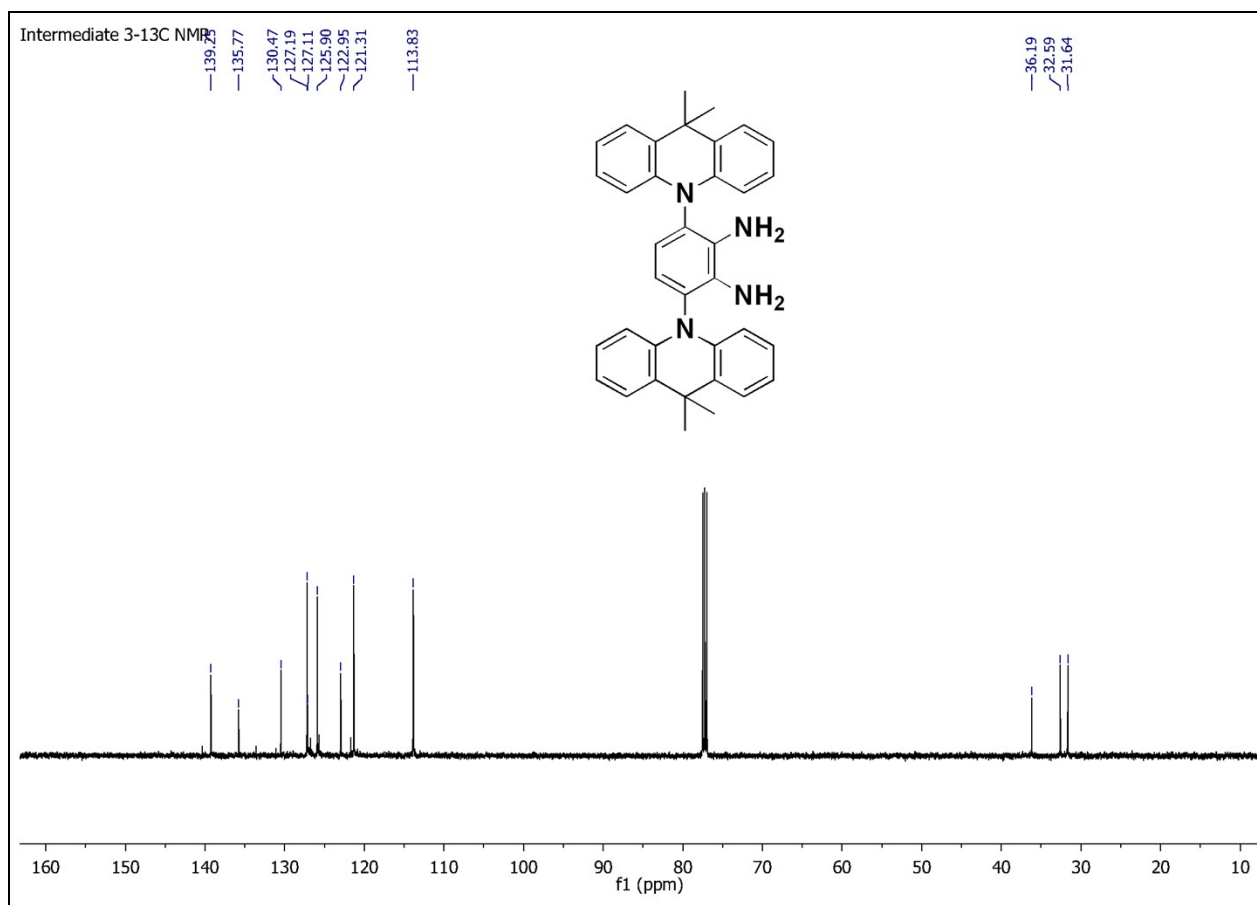


Figure S14. ¹³C NMR spectrum of intermediate 3.

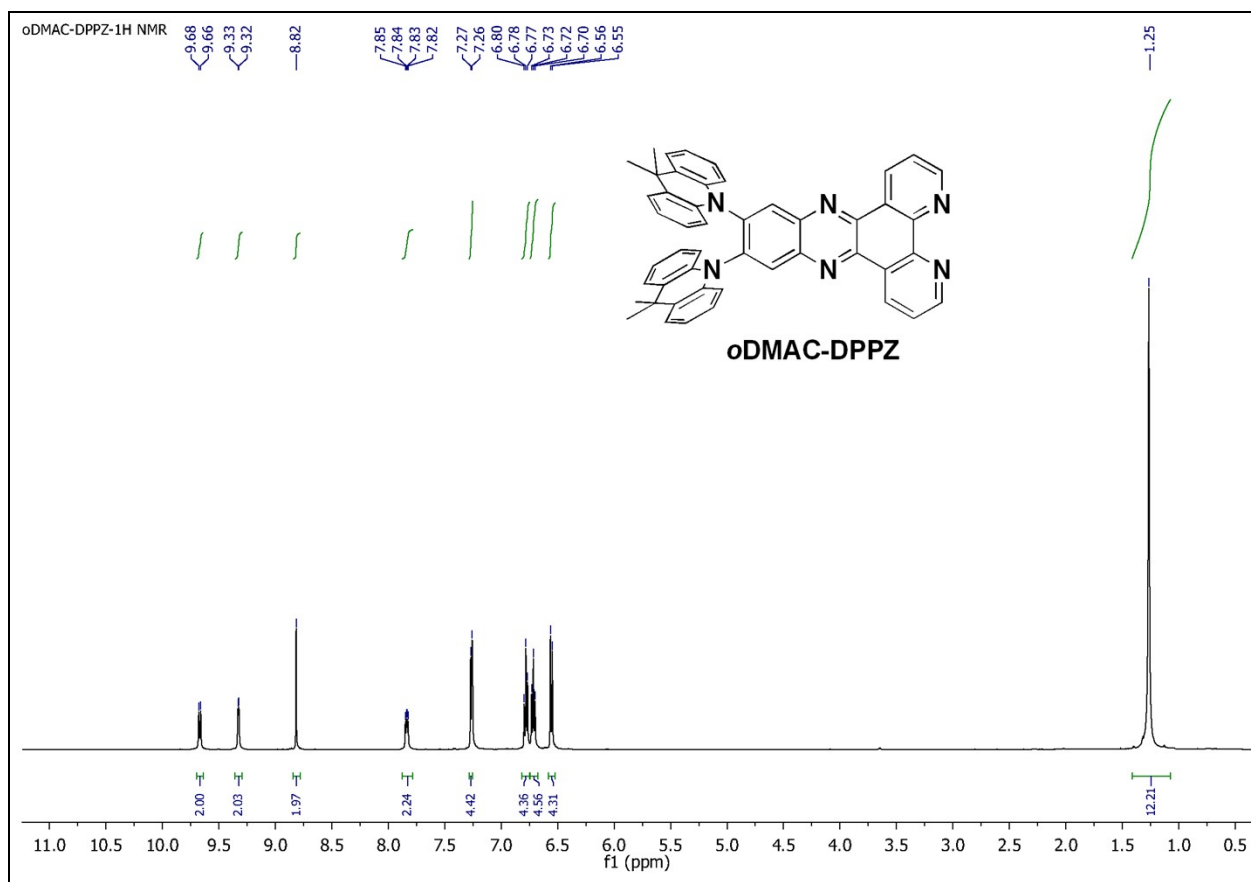


Figure S15. ^1H NMR spectrum of *o*DMAC-DPPZ.

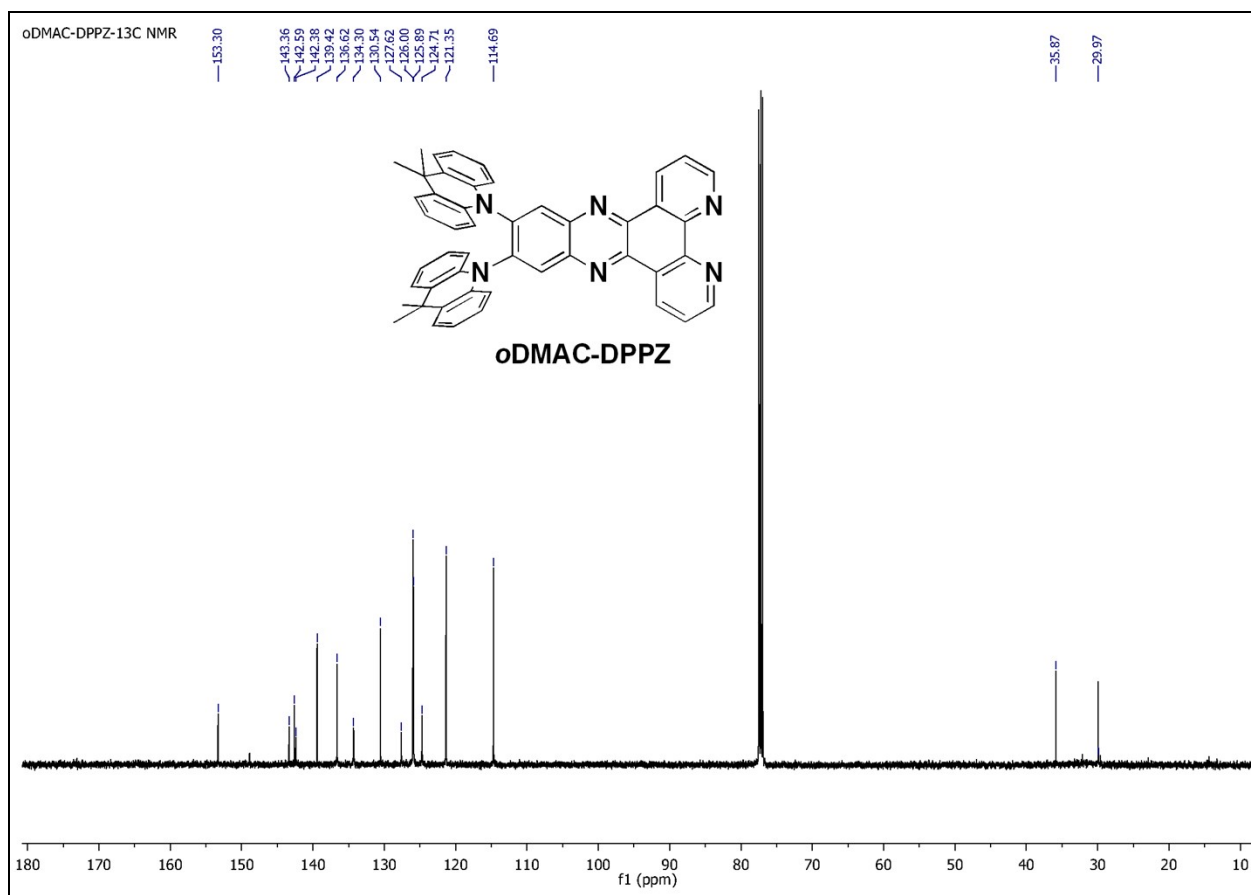


Figure S16. ^{13}C NMR spectrum of *o*DMAC-DPPZ.

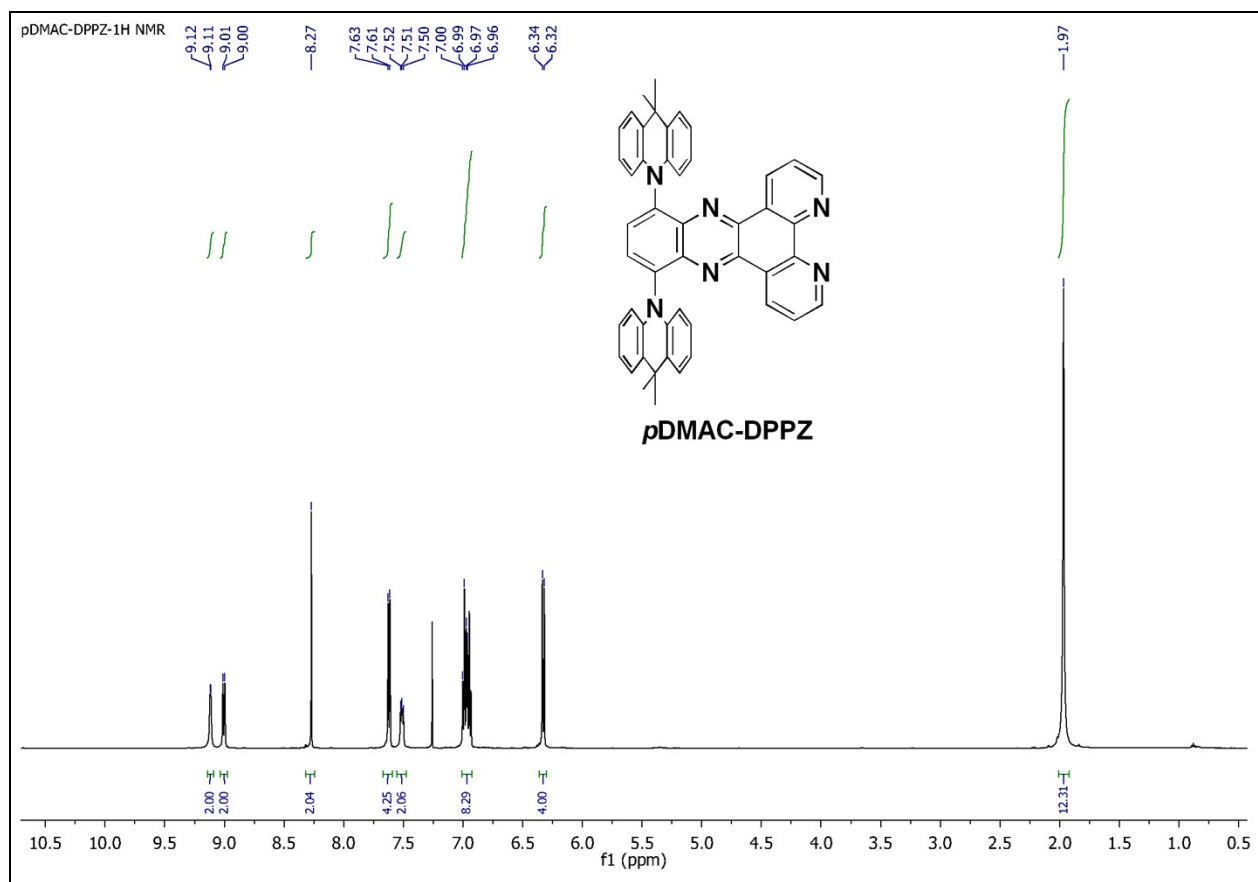


Figure S17. ^1H NMR spectrum of *p*DMAC-DPPZ.

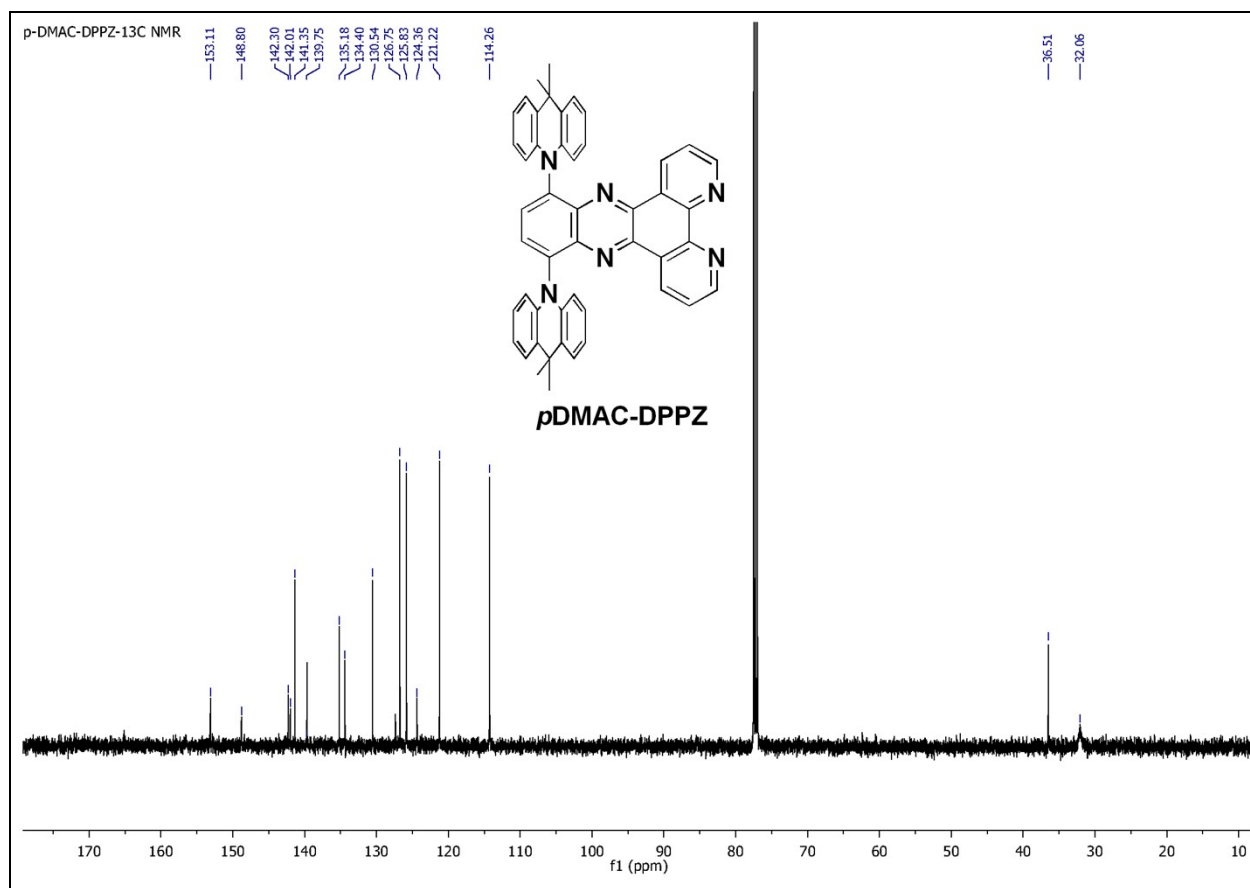


Figure S18. ^{13}C NMR spectrum of *p*-DMAC-DPPZ.